JOURNAL OF SCIENCE
SAKARYA UNIVERSITY

Sakarya University Journal of Science

ISSN 1301-4048 | e-ISSN 2147-835X | Period Bimonthly | Founded: 1997 | Publisher Sakarya University | http://www.saujs.sakarya.edu.tr/en/

Title: The Effect of Thickness on Photocatalytic Performance in MgZnO Thin Films

Authors: Mehmet KURU
Recieved: 2019-11-11 10:28:53

Accepted: 2020-04-15 00:22:58

Article Type: Research Article
Volume: 24
Issue: 4
Month: August
Year: 2020
Pages: 586-595

How to cite
Mehmet KURU; (2020), The Effect of Thickness on Photocatalytic Performance in MgZnO Thin Films. Sakarya University Journal of Science, 24(4), 586-595, DOI: https://doi.org/10.16984/saufenbilder.645104
Access link
http://www.saujs.sakarya.edu.tr/en/pub/issue/55932/645104

Sakarya University Journal of Science 24(4), 586-595, 2020

The Effect of Thickness on Photocatalytic Performance in MgZnO Thin Films

Mehmet KURU*[1]

Abstract

In this study, the effect of thickness of MgZnO thin films which provide high efficiency as photocatalyst under UV light on structural and photocatalytic performance was investigated. For this reason, MgZnO thin films were produced by RF/DC magnetron sputtering technique at room temperature. MgZnO thin films at different thicknesses were deposited on Si (100) substrate and samples were subsequently annealed in the oven at 400 °C for 1 hour. Structural and morphological properties of MgZnO thin films were investigated using the Scanning Electron Microscopy (SEM), Grazing Incident X-ray diffraction (GIXRD) and Atomic Force Microscopy (AFM). All films have hexagonal-wurtzite crystal structure. Also, the crystallite size was 22.95 nm for the 400 nm film and the average crystallite size rised to 35.42 nm with increasing film thickness. The results showed that the structural properties roughness and surface morphology of the films varied depending on the thickness. Also, photocatalytic performances of MgZnO thin films at different thicknesses were measured by UV–Vis spectroscopy. The reaction rate constant (k) for MgZnO photocatalyst with a thickness of 800 nm was calculated as $27.86 \times 10^{-2} s^{-1}$. This result shows that photocatalysts of different thickness suitable with the first-order velocity law because the thin films degradation in the low concentration methylene blue (MB) solution.

Keywords: MgZnO thin films, Magnetron co-sputtering, Photocatalytic performance, Methylene Blue

* Corresponding Author: kurumehmet54@gmail.com
[1] Department of Metallurgy and Materials Engineering, Ondokuz Mayıs University, 55139, Samsun, Turkey
ORCID: https://orcid.org/0000-0001-6030-0791

1. INTRODUCTION

The fact that textile dyestuffs do not break down in nature is one of the major factors that cause pollution of limited drinking water resources. Various organic compounds used as dyes, pesticides, insecticides, phenols and solvents are widely used in industrial applications and in daily life. These substances are mixed with water resources and cause pollution of our natural resources [1,2]. Also, the wastewater generated by the textile industry contains highly toxic aromatic amine compounds and is one of the main causes of environmental pollution [3]. These compounds having a complex aromatic structure are highly resistant to chemicals, light, temperature and other factors. Due to these properties, they cannot be treated efficiently by conventional treatment methods. Recently, Advanced Oxidation Process (AOP) is one of the promising methods for the purification of organic aromatic compounds from wastewater. In this method, exposure of the catalyst or oxidizing compound to UV light or visible light produces hydroxyl radicals on their surfaces. These radical groups attack the bonds of organic pollutants to break them into harmless compounds [4]. The photocatalysis method, which is one of the advanced oxidation processes, promises the future because it is economical and highly efficient than the methods using Ozone and Hydrogen Peroxide [5].

Many of the semiconductor metal oxides have been extensively studied because they retain their stable structure when stimulated by UV and visible light. These can be referred to as Titanium Oxide (TiO_2), Cerium Oxide (CeO_2), Zinc Oxide (ZnO), Tin Oxide (SnO_2), Tungsten Oxide (WO_3) and Zirconium Oxide (ZrO_3) [6,7]. ZnO, which is one of the semiconductor metal oxides, is preferred more than other metal oxides in the removal of organic pollutants due to its anti-bacterial, high quantum yield and environmentally friendly [8]. In addition, since ZnO absorbs much more of the light spectrum than TiO_2 [9], it can break down organic pollutants more effectively. The preparation methods, phase purity, band energy range, surface area, additive and crystal size affect the photocatalytic activity of ZnO [10]. When the band energy range increases, their photocatalytic activity increases because the semiconductor metal oxides occur high-energy electron-hole pairs [11].

Nowadays, the decomposition of dyes as a result of the stimulation of semiconductor metal oxides with UV light is one of the promising treatment methods. ZnO is widely preferred among metal oxides due to its wide band energy and oxidation ability [12]. In addition, ZnO is inexpensive, antibacterial and environmentally friendly, allowing it to stay one step ahead of other photocatalysts and attract more attention [13]. Although ZnO has a high photocatalytic potential [10], its use under high energy UV light is limited due to the narrow band energy range. This narrow band gap is one of the main factors that reduce the photocatalytic activity of ZnO and is one of the most important barriers to its use in commercial applications. In recent studies [7], it has been observed that the addition of elements with different properties to ZnO increases the photocatalytic activity of ZnO by creating band energy gap and surface defects.

The simplest and most convenient method of increasing the band energy range is to add elements to ZnO thin films [11]. Element doping may cause thermal imbalances in the crystal structure. However, it allows the formation of factors that increase the photocatalytic activity in the crystal size and surface area of the films. The doping occurs in two different groups using metal or nonmetallic ions. Metals are preferred as doping elements because they can easy transfer electrons and rise the band energy range [14]. In general, Al, Cu Mg, Ag, Ni, Mn and Co are used as doping elements. [15]. Recently Mg^{+2} (0.57Å) is more preferred than other metals [16] because it has similar radius of ion as Zn^{+2} (0.60Å) and can easily settle into the crystal structure. In addition, it is used in ZnO doping due to its low cost and harmless to the environment [17]. The increase of band energy range with the addition of Mg is due to the Moss-Burstein effect of electrons occurred by oxygen gaps. During doping, Mg^{+2} and Zn^{+2} are replaced by different ionic radius and electronegativity, increasing electron

concentration and oxygen gaps [16]. Also, Mg doping allows the extension of the absorbed wavelength from the UV-A region to the UV-B and UV-C region [17]. The absorbed wavelength and band energy ranges, which are important in photocatalytic applications, can be increased by Mg addition.

Various methods such as RF/DC magnetron sputtering, chemical vapor deposition (CVD), sol-gel, metal organic vapor phase epitaxy (MOVPE), pulsed laser deposition (PLD) and molecular beam epitaxy (MBE) can be used in the production of MgZnO films [18]. Magnetron sputtering method attracts attention due to its easy control deposition rate, chemical composition, film formation [19]. It is also possible to produce materials with different properties by changing the production parameters with this method. Since magnetron co-sputtering method takes place under high vacuum, it enables the production of homogeneous thin films of high purity and quality. Consequently, it is possible to produce films with electrical, optical and magnetic properties that are resistant to corrosion and corrosion [20]. Because of these properties, the co-sputtering method promises future to produce Mg doped ZnO thin films.

2. MATERIALS AND METHODS

MgZnO thin films were coated by RF/DC magnetron co-sputtering technique on Si (100) substrate. The Mg target material has a purity of 99.95% and ZnO has a purity of 99.999%. Substrates was cleaned in the ultrasonic bath with acetone, ethanol and isopropanol respectively for 5 min each and dried with nitrogen. The vacuum chamber was flushed several times with argon to avoid any contamination gas in the chamber, and subsequently purged down to 2×10^{-7} Torr base pressure. We pre-sputtered the targets for 90 min before starting deposition for remove the oxide layer from the surface of the targets. During pre-sputtering, the substrate shutter was kept closed to avoid any contamination of the substrates. 10 W DC power sputtering of Mg and 75 W RF power sputtering of ZnO were used for fabrication of 400 nm, 500 nm, 600 nm, 700 nm, 800 nm and 900 nm MgZnO films. The thickness of the films was measured by the Inficon©-QCM thickness measurement system during the growth process. The deposition was completed in 4mTorr deposition pressure, 0.4 Å/s coating rate and 15 sccm argon gas flow at room temperature. After the deposition of films at different thickness, annealed oxygen atmosphere in the oven at 400 °C for 1 hour.

3. RESULTS AND DISCUSSIONS

After completed fabrication, structural properties were characterized by using (GIXRD) in 2θ range of 20°–80°. Morphological and roughness properties of MgZnO thin films were examined with SEM and AFM. The photocatalytic performance of MgZnO thin films was investigated by degradation of MB solution having a concentration of 1 mmol/ L. The MB solution was irradiated by continuous stirring for 14 hours with a UV lamp of 254 nm wavelength. The differences in absorbance were monitored by UV–Vis spectrophotometer. The XRD spectrum of MgZnO films deposited on Si (100) having a thickness of 400 nm, 500 nm, 600 nm, 700 nm, 800 nm, 900 nm and annealed at 400 ºC is given in Figure 1. As seen from the XRD spectrum, $2\theta = 34.5^{o}$ (002) and $2\theta = 63$ (103) peaks were observed in all films. These peaks confirm that MgZnO thin films of different thickness have hexagonal-wurtzite structure according to the JCPDS 36-1451 [21]. However, low intensity (200) and (111) MgO peaks were also observed in MgZnO films produced at different thicknesses and subjected to heat treatment at 400 °C [22]. The same crystal structure was observed for all films, but the peak full width at half maximum (FWHM) and these peak intensities varied depending on the film thickness. With the increase of film thickness, the peak intensities increased while the FWHM decreased. As the film thickness increases, it is understood that there is a growth race between adjacent crystals relative to the crystal orientation. This competition leads to the growth of crystal faces of the same type to form a free surface. The growth of these crystal surfaces and the decrease in the FWHM by increasing the peak intensity increases the crystalline quality of the films. In MgZnO films deposited at different thicknesses, peak intensities

increased as the thickness increased, while the maximum peak intensity was observed in 800 nm thickness film. After this thickness, peak intensity decreased and (111), (200) MgO peaks became more dominant.

The average crystal sizes (D) of the films were calculated with the help of the Debye-Scherrer equation given by equation 1 [7].

$$D = \frac{0.9\lambda}{\beta cos\theta} \quad (1)$$

In here λ, θ and β are expressed as wavelength of X-ray, Bragg's angle and angular width of peaks at FWHM, respectively. According to the calculations, the crystallite size was 22.95 nm for the 400 nm film and the average crystallite size rised to 35.42 nm with increasing film thickness.

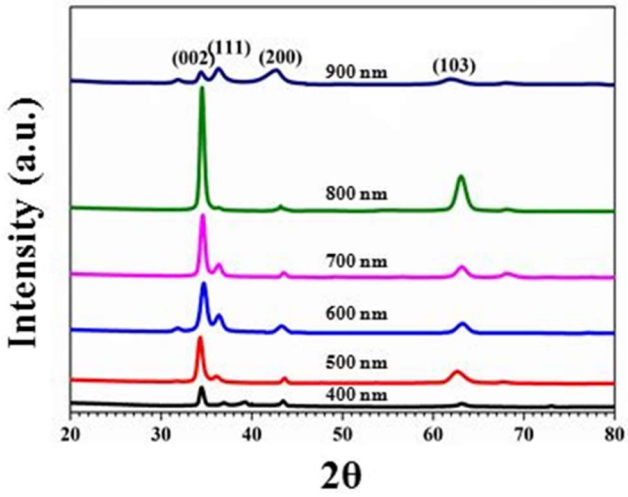

Figure 1. XRD diffraction pattern of MgZnO thin films at different thickness

a, b and c lattice parameters of the hexagonal system are calculated by the equation 2 [23].

$$\frac{1}{d^2} = \frac{4\,(h^2+k^2+hk)}{3a^2} + \frac{l^2}{c^2} \quad (2)$$

In this equation d, (hkl) and a,c expressed as interplanar spacing, miller indices and lattice parameters, respectively. In addition, the volume of the unit cell (V) is calculated using equation 3 [23],

$$V = \frac{\sqrt{3}}{2}a^2c \quad (3)$$

Average crystallite size (D), lattice parameters (a=b, c) and unit cell volumes of MgZnO thin films are given in Table 1. As can be seen clearly in the Table 1, average crystal sizes are different as peak intensities and the FWHM vary depending on thickness. Also, the calculated lattice constants of thin films with different thicknesses are in agreement with the standard values (a=b=3.25Å, c=5.20Å) [24]. This indicates that the films have tensile strength along the c axis for all thicknesses.

Table 1. The peak full width at half maximum (FWHM), Average crystallite size (D), lattice parameters (a = b, c), unit cell volume and Root mean square roughness values of MgZnO thin films

Thickness (nm)	FWHM	D (nm)	a (Å)	c (Å)	V (Å)^3	RMS (nm)
400	0.759	22.92	3.228	5.206	46.978	8.845
500	0.620	28.02	3.271	5.224	48.375	9.674
600	0.569	30.56	3.256	5.163	47.449	9.452
700	0.510	34.08	3.238	5.182	47.052	9.997
800	0.505	34.42	3.237	5.192	47.150	27.916
900	0.750	23.20	3.332	5.212	50.112	14.929

Surface and cross-sectional SEM images of MgZnO thin films with different thicknesses and annealed at 400 °C are given in Figure 2. When the surface SEM images are examined, it is seen that the substrate surface is completely homogeneously and uniformly coated with MgZnO particles. It is also clear that film thickness has a large effect on surface morphology. SEM results show that coating thickness can directly affect crystal growth, grain boundary amount and grain size of films, which can play an important role in photocatalytic properties. The MgZnO film, which has a thickness of 400 nm, consists of fine-grained structures, and as the thickness increases, the grains combine to form coarse-grained structures. The largest grains were observed in the 800 nm

film, while the 900 nm film reduced the grain size. The results obtained from the SEM images agree with the XRD calculations. EDX analysis of MgZnO thin films is given in Table 2.

Table 2. EDX results of MgZnO thin films

Atomic (%)	Film Thickness (nm)					
	400	500	600	700	800	900
Zn	33.74	40.02	44.08	43.12	40.79	42.08
O	54.36	49.28	45.21	46.17	45.52	47.21
Mg	11.90	10.70	10.71	10.71	13.69	10.71

When the EDX results were examined, no impurity peaks were observed for each film except Zn, O and Mg. In addition, Mg ratios in all films are very close to each other. These results show that Mg is successfully added to ZnO by RF/DC magnetron sputtering method simultaneously.

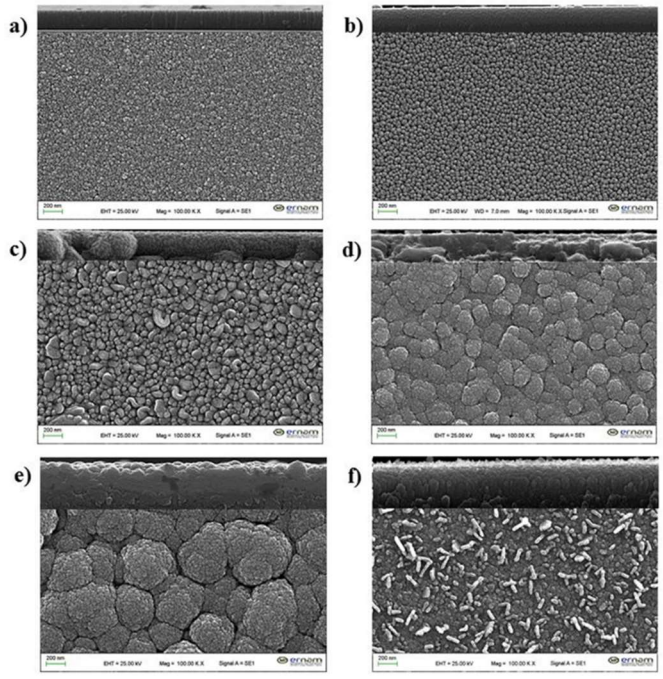

Figure 2. SEM images of MgZnO thin films. a) 400nm, b) 500nm, c) 600nm, d) 700 nm, e) 800 nm and f) 900 nm

The change of surface roughness of MgZnO thin films depending on film thickness was examined by atomic force microscopy. 3D AFM images of 5x5 μm^2 dimensions of MgZnO thin films of different thicknesses are given in Figure 3 and the root mean square (RMS) values are given in Table 1. As shown in Figure 3, 400 nm thick film is composed of small grains and RMS value is 8.845 nm. As the film thickness increased, the small grains joined to form larger grains and RMS value increased. The highest surface roughness was observed in 800 nm thickness film with 27.916 nm value. With increasing film thickness, the increase in RMS roughness is sourced from the larger grain formation as well as the increase in porosity of the films [25]. Also, RMS roughness values were increased with film thickness similar to the average crystal sizes obtained from XRD results.

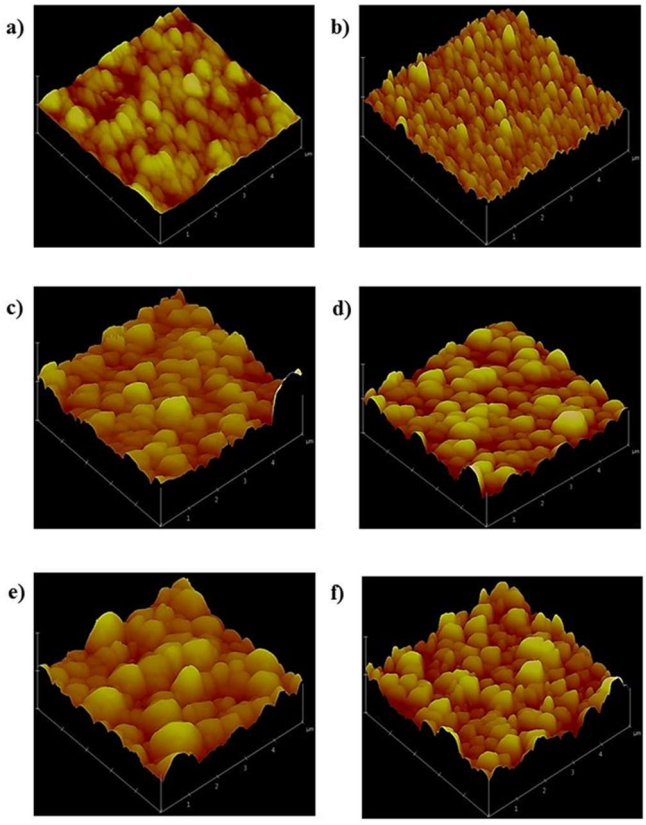

Figure 3. 3D AFM images of MgZnO thin films. a) 400nm, b) 500nm, c) 600nm, d) 700 nm, e) 800 nm and f) 900 nm.

In MgZnO film with a thickness of 900 nm, peak intensity, average crystal size and surface roughness were reduced as in XRD results. The change of grain sizes and surface fluctuations can explain the difference in RMS roughness of thin films. In films with high surface roughness, we

think that photocatalytic performance increases because the surface area increases. [26]

3.1. Photocatalytic performance

In the photocatalysis method, when the photocatalyst is irradiated with a high energy light, the electrons in the valence band (VB) are transferred to the conductivity band (CB). Thus, electron holes (h^+) are occurred in the VB. The holes obtained radical OH^- groups by oxidizing the water molecules on the photocatalyst. These OH^- groups convert organic dyes to harmless form. As the increased electron density in the conductivity band decreases the amount of negatively charged oxygen by increasing the amount of dissolved oxygen [27], the degradation rate also increases [28].

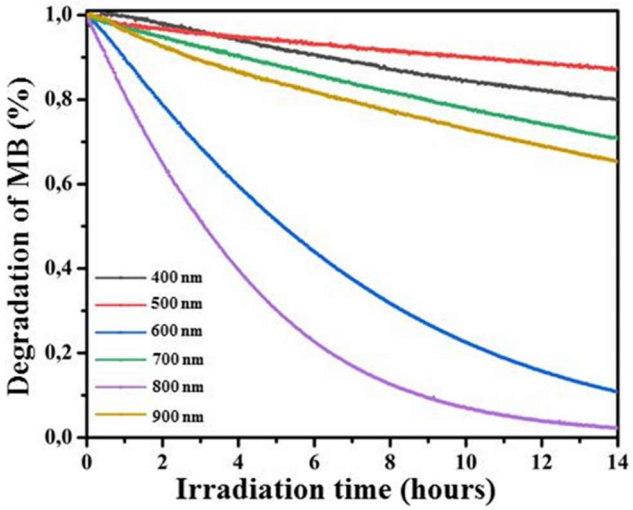

Figure 4. Comparison of time dependent degradation rate of MB for MgZnO thin films

The photocatalytic performance of the MgZnO thin films was calculated by degrading MB by stimulating with a 254 nm wavelength UV lamp. MgZnO thin films with different thickness of UV light irradiation time versus the degradation rate of MB is given in Figure 4. In the MgZnO photocatalyst with a thickness of 500 nm, the degradation rate of MB was 14%, while the 800 nm thickness photocatalyst was 99%. The degradation rate of MB for MgZnO photocatalysts is given in Table 3. As seen in Table 3 and Figure 4, there is no linear relationship between film thickness and degradation. In other words, as the film thickness increased, there was no increase in the rate of degradation. While the maximum degradation of MB was observed in MgZnO photocatalyst having a thickness of 800 nm with 99% ratio, almost all the dyes were degraded. When the degradation rates are compared with the average grain size and surface roughness values, the results are in agreement with each other. The best results were obtained in 800 nm thickness MgZnO thin film.

Table 3. The degradation rate of MB and kinetic rate constant values for MgZnO photocatalysts

Thickness (nm)	Degradation rate of MB (%)	Kinetic rate constants (k, s^{-1}) (10^{-2})
400	21	1.52
500	14	0.86
600	89	17.34
700	30	2.43
800	99	27.86
900	35	2.92

While the maximum degradation of MB was observed in MgZnO photocatalyst having a thickness of 800 nm with 99% ratio, almost all the dyes were degraded. When the degradation rates are compared with the average grain size and surface roughness values, the results are in agreement with each other. The best results were obtained in 800 nm thickness MgZnO thin film.

In order to determine the photocatalytic performance of MgZnO thin films, reaction kinetics of degradation were investigated. To define the kinetics of photocatalytic degradation, several models have been developed such as zeroth-order velocity law, the first-order velocity law, and the parabolic diffusion model [29]. In

diluted solutions, the reaction takes place in accordance with the first order kinetics given by Eq.4,

$$ln\left(\frac{C}{C_o}\right) = -kt \quad (4)$$

In this equation C is the concentration after reaction, C_o initial concentration, k reaction rate constant and t UV irradiation time. The time-dependent ln(C/C$_o$) graph for MgZnO films is given in Figure 5. The kinetic rate constant (k) values calculated from the slope of Figure 5 are given in Table 3.6.

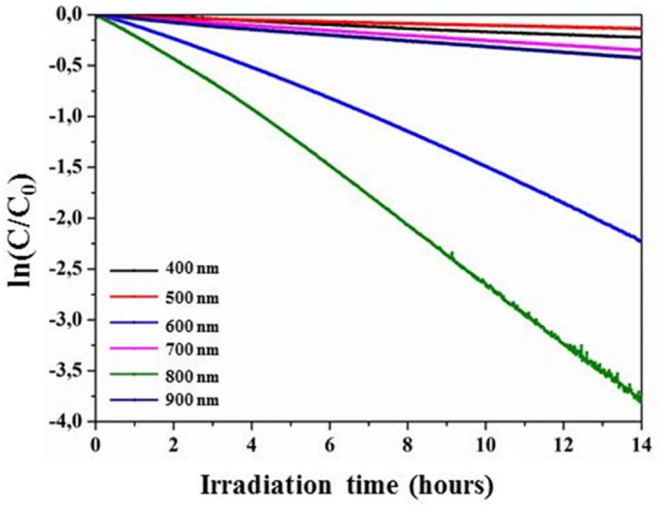

Figure 5. The time-dependent ln(C/C$_o$) graph for MgZnO films

The kinetic rate constant (k) for the MgZnO photocatalyst with a thickness of 500nm was $0.86x10^{-2}s^{-1}$, while the value for the film with a thickness of 800 nm was calculated as $27.86x10^{-2}s^{-1}$, and the reaction rate constant value increased almost 30 times. Some factors such as crystallinity, crystal orientation and surface area affect the photocatalytic performance of MgZnO thin films [30]. For MgZnO photocatalysts of different thickness, degradation of MB at low concentrations indicates that it is suitable with the first-order velocity law.

4. CONCLUSIONS

In order to rise the photocatalytic performance of ZnO, MgZnO thin films with different thicknesses were produced by RF/DC magnetron sputtering technique. When XRD results are examined, (002) and (103) peaks seen in films with different thicknesses indicate that MgZnO films are hexagonal wurtzite-type structure. The effect of thickness on photocatalytic performance was investigated by degradation of MB solution. The lowest photocatalytic performance was observed in a film having a thickness of 500 nm with a degradation rate of 14%, while the best performance was observed in a film having a thickness of 800 nm with rate 99%. As a result of the experiments, it was observed that the thickness did not have a linear effect on photocatalytic performance. But although there is no linear ratio, MgZnO photocatalysts of different thickness suitable with the first-order velocity law because the thin films degradation in the low concentration MB solution.

Acknowledgements

This work is in supported by TUBITAK (Scientific and Technical Research Council of Turkey) Project Number 217M236.

Research and Publication Ethics

The author declares that all the information in this paper is accurate and completely correct that he has behaved in accordance with the scientific ethic in the course of the production of the information and cited all the sources that he has used.

Ethics Committee Approval

This paper does not require any ethics committee permission or special permission.

Conflict of Interests

The author declares that he has no known competing financial interests or personal relationships that could have appeared to influence the work reported in this paper.

REFERENCES

[1] M. Grassi, G. Kaykioglu, V. Belgiorno and G. Lofrano, "Removal of emerging contaminants from water and wastewater by adsorption process, in Emerging Compounds Removal from Wastewater: Natural and Solar Based Treatments," ed. by G. Lofrano, Springer, Dordrecht, 2012.

[2] K. Kümmerer, "The presence of pharmaceuticals in the environment due to human use—present knowledge and future challenges," Journal of Environmental Management, vol. 90, pp. 2354–2366, 2009.

[3] T. Robinson, G. McMullan, R. Marchant and P. Nigam, "Remediation of dyes in textile effluent: a critical review on current treatment technologies with a proposed alternative". Bioresource Technology, vol. 77, pp. 247-255, 2001.

[4] H. Lachheb, F. Dappozze, A. Houas and C. Guillard, "Adsorption and photocatalytic degradation of cysteine in presence of TiO_2", Journal of Photochemistry and Photobiology A: Chemistry, vol. 246, pp. 1-7, 2012.

[5] Y. Deng and R. Zhao, "Advanced oxidation processes (AOPs) in wastewater treatment," Current Pollution Reports, vol. 1, pp. 167–176, 2015.

[6] A. Ibhadon and P. Fitzpatrick, "Heterogeneous photocatalysis: recent advances and applications," Catalysts, vol. 3, pp. 189-218, 2013.

[7] M. Kuru and H. Narsat, "The effect of heat treatment temperature and Mg doping on structural and photocatalytic activity of ZnO thin films fabricated by RF magnetron co-sputtering technique," Journal of Materials Science: Materials in Electronics, vol. 30, pp. 18484–18495, 2019.

[8] W. Bolong, Y. Fucheng, L. Haishan, S. Tianyun, N. Dongmei, H. Ling, D. Hongyan, W. Shu and X. Tang, "The preparation and photocatalytic properties of Na doped ZnO porous film composited with Ag nano-sheets", Physica E: Low-dimensional Systems and Nanostructures, vol. 117, pp. 113712, 2020.

[9] O. D. M. Navarro and J. L. Sánchez-Salas, "Focus on Zinc Oxide as a Photocatalytic Material for Water Treatment", International Journal of Bioremediation & Biodegradation, vol. 116, 2018.

[10] S. Chakrabarti and B.K. Dutta, "Photocatalytic degradation of model textile dyes in wastewater using ZnO as semiconductor catalyst," Journal of Hazardous Materials, vol. 112, pp. 269–278, 2004.

[11] S. Suwanboon, P. Amornpitoksuk, P. Bangrak and N. Muensit, "Optical, photocatalytic and bactericidal properties of $Zn_{1-x}La_xO$ and $Zn_{1-x}Mg_xO$ nanostructures prepared by a sol–gel method," Ceramics International, vol. 39, pp. 5597–5608, 2013.

[12] D. R. Kumar, K.S. Ranjith, L.R. Nivedita, K. Asokan and R.T. Rajendra Kumar, "Swift heavy ion induced effects on structural, optical and photo-catalytic properties of Ag irradiated vertically aligned ZnO nanorod arrays", Nuclear Instruments and Methods in Physics Research B, vol. 450, pp. 95–99, 2019.

[13] A. Ziashahabi, M. Prato, Z. Dang, R. Poursalehi and N. Naser, "The efect of silver oxidation on the photocatalytic activity of Ag/ZnO hybrid plasmonic/metal-oxide nanostructures under visible light and in the dark", Scientific Reports, vol. 9, pp. 11839, 2019.

[14] M.R.D. Khaki, M.S. Shafeeyan, A.A.A. Raman and W. Daud, "Application of doped photocatalysts for organic pollutant degradation-a review," Journal of Environmental Management, vol. 198, pp. 78–94, 2017.

[15] K. Verma, B. Chaudhary, V. Kumar, V. Sharma and M. Kumar, "Investigation of structural, morphological and optical properties of Mg:ZnO thin films prepared by sol-gel spin coating method," Vacuum vol. 146, pp. 524–529,2017.

[16] T.B. Ivetić, M.R. Dimitrievska, N.L. Finčur, L.R. Đačanin, I.O. Gúth, B.F. Abramović and S.R. Lukić-Petrović, "Effect of annealing temperature on structural and optical properties of Mg-doped ZnO nanoparticles and their photocatalytic efficiency in alprazolam degradation," Ceramics International, vol. 40, pp. 1545-1552, 2014.

[17] V. Etacheri, R. Roshan, and V. Kumar, "Mg-doped ZnO nanoparticles for efficient sunlight-driven photocatalysis," ACS Applied Materials & Interfaces, vol. 4, pp. 2717-2725, 2012.

[18] C. Abed, C. Bouzidi, H. Elhouichet, B. Gelloz and M. Ferid, "Mg doping induced high structural quality of sol–gel ZnO nanocrystals: application in photocatalysis," Applied Surface Science, vol. 349, pp. 855–863, 2015.

[19] M. Kuru, A. E. Özmetin, A. Özmetin and O. Şahin, "The role of heat treatment on the structural and nano-mechanical properties of $SmCo_5$ thin films grown by RF magnetron sputtering technique," Ceramics International, vol. 43, pp. 3893-3899, 2017.

[20] S. Youssef, P. Combette, J. Podlecki, R. Al Asmar, and A. Foucaran, "Structural and optical characterization of ZnO thin films deposited by reactive rf magnetron sputtering", Crystal Growth & Design, vol. 9, pp.1088–1094, 2008.

[21] C. Liua, F. Shang, G. Pan, F. Wang, Z. Zhou, W. Gong, Z. Zi, Y. Wei, X. Chena, J. Lv, G. He, M. Zhang, X. Song and Z. Sun, "Preparation and photocatalytic activity of $Mg_xZn_{1-x}O$ thin films on silicon substrate through sol–gel process," Applied Surface Science, vol. 305, pp. 753–759, 2014.

[22] S. K. Mahadeva, J. Fan, A. Biswas, K. S. Sreelatha, L. Belova, and K. V. Rao, "Magnetism of Amorphous and Nano-Crystallized Dc-Sputter-Deposited MgO Thin Films", Nanomaterials, vol. 3, pp. 486-497, 2013.

[23] A. H. Hammad, M. Sh Abdel-Wahab, S. Vattamkandathil and A. R. Ansari, "Structural and optical properties of ZnO thin films prepared by RF sputtering at different thicknesses," Physica B, vol. 540, pp. 1–8, 2018.

[24] B.D. Cullity and C.D. Graham, "Introduction to Magnetic Materials" Wiley, Hoboken, 2009.

[25] V. Kumar, N. Singh, R.M.Mehra, A. Kapoor, L.P.Purohit and H.C.Swart, "Role of film thickness on the properties of ZnO thin films grown by sol-gel method", Thin Solid Films, vol. 539, pp. 161-165, 2013.

[26] J. Lv, W. Gong, K. Huang, J. Zhu, F. Meng, X. Song and Z. Sun, "Effect of annealing temperature on photocatalytic activity of ZnO thin films prepared by sol–gel method", Superlattices and Microstructures, vol. 50, pp. 98-106, 2011.

[27] M. A. Rauf and S. S. Ashraf, "Fundamental principles and application of heterogeneous photocatalytic degradation of dyes in solution", Chemical Engineering Journal, vol. 151, pp. 10-18, 2009.

[28] Z. Wang, C. Chen, F. Wu, B. Zou, M. Zhao, J. Wang and C. Feng, "Photodegradation of rhodamine B under visible light by bimetal co-doped TiO_2 nanocrystals," Journal of Hazardous Materials, vol. 164, pp. 615–620 2009.

[29] Zhaohui Li, "Sorption kinetics of hexadecyltrimethylammonium on natural clinoptilolite," Langmuir, vol. 15, pp. 6438–6445, 1999.

[30] N. M. Flores, U. Pal, R. Galeazzi, and A. Sandoval, "Effects of morphology, surface

area, and defect content on the photocatalytic dye degradation performance of ZnO nanostructures," RSC Advances, vol. 4, pp. 41099-41110, 2014.